Broadband Evolutionary Optimisation of a Free Form Contour Defined Serrated Edge Compact Antenna Test Range

M. Dirix [1], S.F. Gregson [2, 3]
[1] Antenna Systems. Solutions, Santander, Spain; mdirix@asysol.com
[2] Next Phase Measurements LLC, CA, USA
[3] Queen Mary University London, London, UK

***Abstract*—Modern evolutionary optimization techniques when used with efficient parallelized electromagnetic simulation algorithms provide a very effective strategy for the design of high-performance compact antenna test ranges that can be readily tailored to address specific measurement needs. This paper extends the authors previous studies to include far more general serrated edge reflector designs than have previously been considered that, for the first time, not only refine the serration profile, but also the envelope of the projected outline of the offset parabolic reflector. This paper presents results that illustrate the utility of this approach examining and comparing fully broadband optimized predicted CATR quiet-zone performances.**

Index Terms— CATR, antenna measurement, serrated edge, genetic optimization, superformula, squircle, 5G

I. INTRODUCTION

The Compact Antenna Test Range (CATR) comprising a low gain feed illuminating an offset parabolic reflector is a very widely used approach for taking far-field antenna measurements at fixed range lengths that are very much less than those distances suggested by the Rayleigh far-field criteria [1]. Thus, the low-gain feed radiates a quasi-spherical wave which is, upon reflection by the parabolic reflector, transformed into a pseudo-TEM, *i.e.* plane, wave that propagates through the region of space in which the test antenna is situated. Early workers quickly identified that controlling and minimising the amount of field diffracted from the edges of the range reflector and that impinges into the zone that is used to test a given antenna under test (AUT) was crucial to the success of the measurement technique [1]. During the past fifty or so years since the first inception of this reduced range length far-field measurement test technique, two contrasting approaches to managing reflector edge diffraction have come to prominence. These are CATRs with serrated edge (SE) reflectors, and CATRs with blended rolled edge (BRE) reflectors where it has been shown that, [2], the quiet-zone (QZ) performance of CATR serrated edges are to rolled edges as Chebyshev filters are to Butterworth filters, *i.e.* more pass-band ripple but with a faster roll off. Although other options are available [1], they are generally far less commonly encountered.

A distinguishing feature of any reflector that is operated as a field collimator is that it is necessarily large in size, both physically where it must be larger than the test article; and electrically where it must be many wavelengths across so that the geometrical optics principle of its operation is realised. This then, when taken in concert with the need for the application of a potentially comparably large reflector edge treatment means that CATR reflectors, and the chambers in which they are situated, can become excessively large, and correspondingly expensive. Thus, the need to produce a well-behaved pseudo-plane-wave, with the requisite degree of quiet-zone uniformity with which to illuminate the test antenna tends to place limits on the lowest frequency of operation for these test systems [1], [2]. Hence, utilising the smallest possible reflector and edge treatment is clearly of the utmost importance, and this is especially so when considering that the total reflector size can, in many instances, be as much as three times the size of the QZ. Thus, the use of modern evolutionary optimization techniques coupled with fast, efficient, parallelized electromagnetic simulation algorithms provides an efficient strategy for exploring the entirety of the design space. This strategy has been successfully harnessed for the design of both serrated edge [3] and blended rolled edge CATRs [2], [4], [5], which as well details the applied simulation and optimization method exhaustively. In this paper however, we will concentrate upon the serrated edge treatment where more general serration designs and reflector shapes are considered than has previously been possible. The organisation of this paper is as follows: Section II provides an overview of the novel parameterised formulation for the reflector edge treatment; Section III presents the results of a recent design campaign that illustrated the effectiveness of the approach and how it has been extended to consider multi-frequency optimizations. Finally the the paper concludes in Section IV.

II. FULL FREE FORM CONTOURS

In [3], it was previously shown that the functional form of a serration used as the edge treatment of a CATR reflector can be effectively expressed using a generalisation of the super-ellipse [6]. In that research it was chosen such that only the outline shape of a single serration was dictated by the Superformula with this then being duplicated to cover all sides of the reflector, in combination with a general

formulation of their respective base width and angle which depended upon the lateral position. However, it was quickly recognised that the Superformula itself allows for a far more flexible description covering the full exterior boundary of the serrated edge reflector. The Superformula [6] is a function that can be used to express a variety of complex curves using only a relatively small number of parameters. This generalisation of the Lamé curve [6] can be written in polar form as,

$$r_{\mathrm{sf}}(\varphi) = \left(\left| \frac{1}{a} \cos\left(\frac{m}{4}\varphi\right) \right|^{n_2} + \left| \frac{1}{b} \cos\left(\frac{m}{4}\varphi\right) \right|^{n_3} \right)^{-\frac{1}{n_1}} \quad (1)$$

Here, m denotes the number of rotational symmetries, which gives the serration count and is forced to positive integer values only, both a and b are radial scaling factors, and n_1, n_2, n_3, define the radial shape, *e.g.* serration outline.

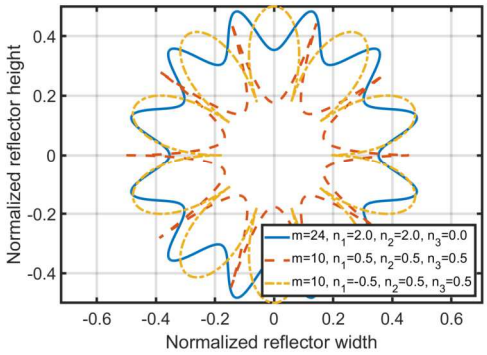

Fig. 1. Example of the use of the superformula for serration design.

Figure 1 illustrates the variation of the reflector edge treatment generated by changing the parameters of the Superformula. Here, it can be seen that a very wide variation in serration shape is possible. Using the now fully validated genetic optimization technique presented in [2], [3], [4] and [5] the optimal serrated reflector contour may be researched more completely. In Figure 2 below, the results of the optimization are shown for a corner offset fed reflector design. For the optimization a maximum width and height in which the reflector is required to fit was imposed, and fixed for the duration of the optimisation, otherwise the optimizer was allowed free reign to use the area within the boundaries in whatever way proved successful from an evolutionary standpoint. It can be seen that these results shown an unexpectedly strong ripple in the centre of the QZ. The strong ripple is expected to arise from the inherent rotational symmetry of this reflector type. Even though in [7] it was shown that a circular reflector can be effectively implemented, here, the strong constructive or destructive interference made this geometry ill-suited for this application. It is noted here, however, as well that these optimization calculate the field as measured by an Hertzian dipole probe, which provides worse case results for the expected QZ performance as in real QZ field probe measurements typically a SGH is employed which inherently employs spatial averaging of the QZ ripple. Although not shown here as a consequence of available space in this paper, inspection of the phase function showed a similar behaviour in the centre of the QZ.

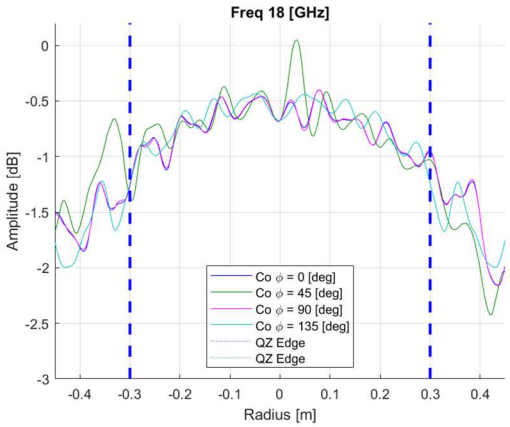

Fig. 2. Quiet Zone performance after genetic optimization of the reflector contour.

Generally, the approach taken by industry is to utilise a broadly rectangular, or square, shaped main body of the reflector having serrations evenly distributed on all sides. Here, we may obtain a similar geometry through the superposition of the Superformula generated serrations on top of a rectangular baseline shape. As the Superformula is defined in polar coordinates, a polar description of rectangle is researched as well.

One of these rectangular-like shapes is the Fernandez-Guasti squircle [8], which we shall henceforth refer to as a "squircle". The squircle is a low degree quartic plane algebraic curve which allows intermediate shapes between an ellipse and a rectangle with the degree being determined by a single, positive valued, scalar parameter. The squircle can be described in polar format as,

$$r_{\mathrm{sq}}(\varphi) = \left(\frac{a\cos\varphi}{2\sqrt{1-s\sin^2\varphi}} + \frac{b\sin\varphi}{2\sqrt{1-s\sin^2\varphi}} \right)^{\frac{1}{2}} \quad (2)$$

Here, s is a parameter that may vary such that $0 \le s \le 1$. When $s = 0$ the shape is an ellipse with major and minor axis a and b respectively. When $s = 1$ the shape is a rectangle with width a, and height b, and in between it is a two-dimensional curve that resembles the circle and the square.

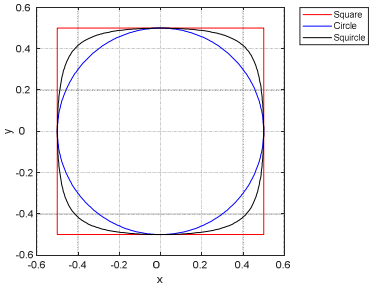

Fig. 3. Illustration of squircle shape variations.

In Figure 3 the range allowed by the squircle algebraic formulation is shown. It is noted here that even though at the

limit the squircle becomes a square, the equation itself results in a division error, thus practically s is limited to $0 \leq s \leq 0.928$ *cf.* [8]. Thus, the final reflector boundary can then be simply calculated from the superposition of both the Superformula serration boundary and the squircle solid reflector boundary as,

$$r(\varphi) = r_{\mathrm{sf}}(\varphi) + r_{\mathrm{sq}}(\varphi) \tag{3}$$

As before, the optimizer is limited in the maximum width and height that the reflector is permitted to occupy during the optimization. Furthermore, the width and height of the squircle are also fixed, resulting in a fixed size solid body and fixed length serrations. Lastly, under the assumption of a cylindrical QZ, the reflector is forced into a circular-square shape, having $a = b$ in Equation (2). The parameter s is added to the list of optimisation parameters thereby allowing the reflector to vary between a "circular" and a "square" envelope.

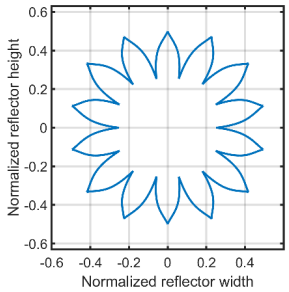

Fig. 4. Optimized reflector boundary

In Figure 4 the reflector boundary after optimization is shown. It can be seen that the inside boundary is now squircle shaped being a square with rounded corners. In Figure 5 the result of the optimization is shown at 18 GHz. While comparing these results with the Superformula boundary results in Figure 2 it can be clearly seen that breaking the rotational symmetry spreads more evenly the diffraction effects, *i.e.* the ripple, across the QZ and thus results in very encouraging CATR QZ performance. It is also noted here, that even though *no* a priori limitation is imposed on the final serration outline, it can be clearly seen that based purely upon the CATR QZ performance, the optimizer greatly favours a "cosine" type shape that is very similar to the those shown in [7].

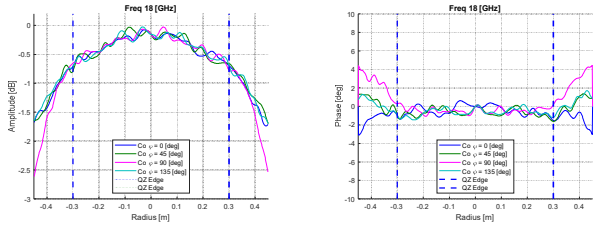

(a) (b)

Fig. 5. Optimization result Superformula serrations with Squircle solid body, (a) amplitude and (b) phase.

This shows that the combination Superformula with squircle base outline already provides very encouraging results with the benefit that only a single optimisation parameter need be included within the evolutionary optimisation process thereby offering advantages in terms of efficiency within the design process. As we already noted, unless the reflector illumination is carefully controlled, the rotational symmetry of the reflector edge tended to produce a ripple inside the QZ and that this phenomena can be softened by forcing the reflector envelope into a more rectangular, *i.e.* squircular shape. This suggests that there may be other profiles that are perhaps even more optimal shapes which define the boundary between the reflector solid body and the serrations. To investigate this further, the squircle boundary in Equation (3) was replaced by a second Superformula shaped boundary. This resulted in the total boundary outline,

$$r(\varphi) = r_{\mathrm{sf},1}(\varphi) + r_{\mathrm{sf},2}(\varphi) \tag{4}$$

It can be shown that for the Superformula similarly as the squircle ellipses and rectangles can be derived, however the Superformula is not limited to *just* those primitives. In this case, the same boundary conditions have been applied as to the optimization of the combined Superformula-Squircle reflector, however the optimization parameter s of the squircle has been replaced by the requisite Superformula parameters with appropriate constraints, *i.e.* $m \in \mathbb{Z}, 3 \leq m \leq 6$, $1 \leq n_1 \leq 30$, $1 \leq n_2 \leq 30$ and $n_3 = n_2$.

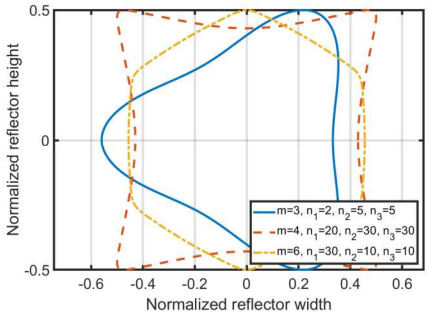

Fig. 6. Superformula generated solid body boundary

In Figure 6 some of the possible variations are shown which can be generated with the Superformula resulting from the parameter space indicated above illustrating the range of potential CATR reflector envelopes that fall within the search space. The genetic optimisation was repeated using this definition of the reflector edge with all other parameters being held consistent to enable a direct comparison to be made. Following this optimisation, the resulting reflector boundary and the boundary of the solid body can be seen presented in Figure 7. Again, encouragingly, the serration outline resembles closely the cosine shape. Interestingly, it can also be seen that given again full freedom, a square-like shape is the preferred shape with less ($m = 3$) or more ($m = 5$, 6) rotational symmetries. It is furthermore interesting to see that it breaks up further any straight lines, but only marginally so. It is also of note that the solid body contour bears a striking resemblance to the junction contour that is routinely used to define the change in profile from the parabolic to the blended rolled sections of a blended rolled edge CATR [1], [5].

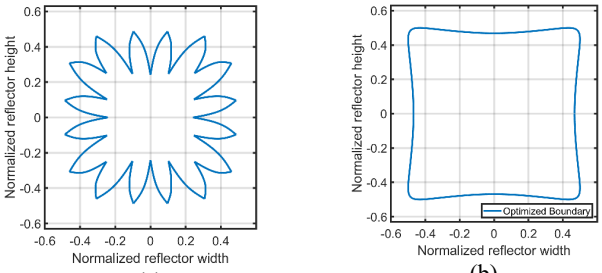

Fig. 7. Optimization result Superformula serrations with Superformula solid body, (a) reflector outline (b) solid body outline

In Figures 9-a and –b, the CATR QZ amplitude and phase results are shown for the Superformula serrations with Superformula solid body boundary. From inspection of the 18 GHz results it can be seen they are very similar to the squircle based results presented above.

While comparing Figure 7(a) with a realized standard reflector product as shown in Figure 8 below, one notices that the optimized reflector outline does not differ too much from an existing serrated edge design, giving further confidence. However, it is also noticed that for the given optimization at 18 GHz, the optimizer prefers a lower serration count. Thus in the next section the broad band behaviour of the design is investigated and further optimized.

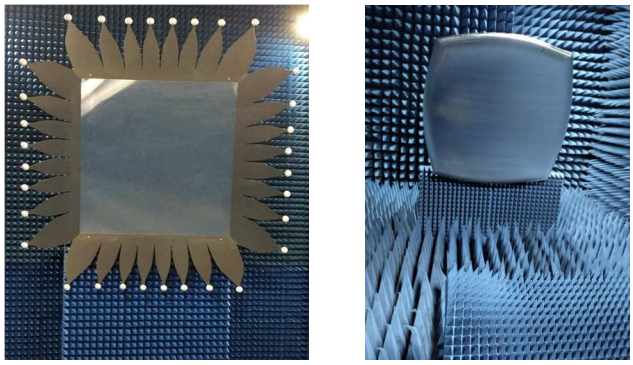

Fig. 8. Installed serrated (left) and blended rolled edge (right) reflector

III. BROADBAND OPTIMIZATION

In the last section it was found by comparison that the reflector optimized at 18 GHz had fewer serrations that would perhaps be the usual, thus the broadband behaviour of the optimized reflector was researched.

In Figures 10-a and -b the amplitude and phase behaviour of the QZ is shown at 8, 18 and 40 GHz for the case where the reflector was optimized at 18 GHz. Here, it can be seen that at 40 GHz an increase in amplitude- and phase-ripple is observed, which indicates that a broadband performance of this reflector was perhaps not ideal. Here, it was suspected that the limited number of serrations caused by the lower optimization frequency may be causing this effect. Thus, a second optimization at 40 GHz was employed to see the difference. Figure 9 shows the difference in reflector outline between the optimization at 18 GHz and 40 GHz. Here, it can be seen that indeed the 40 GHz optimization shows an increased number of serrations, but simultaneously shows a reduction in the length of the serrations. This can be explained by the fact that serrations only need to be a certain multiple of the wavelength in length to operate, after which further increasing length of the serrations provides only a limited improvement in the QZ performance. Thus, the optimization at 40 GHz prefers a larger solid portion of the reflector instead, which has a clear improvement in the phase behaviour within the QZ (*e.g.* Figure 10-d at 40 GHz). However, this is brought at the expense of poorer QZ performance at lower frequencies (*e.g.* Figure 10-c and -d at 8 GHz).

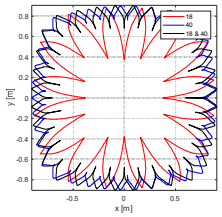

Fig. 9. Free form reflector outline optimized 18, 40 and both 18&40 GHz

Based on these results it can be concluded that as opposed to the previously publish work on the blended rolled edge reflector [2], Figure 8 (right), for the free form contour serrated edge reflector it makes sense to perform a full multi-frequency optimization. Thus the reflector was optimized once more at 18 and 40 GHz simultaneously. It should be noted that these two frequencies have been chosen to roughly span the conceived primary operational frequencies of this CATR, and that the optimizer was setup to give equal priority to the performance of the QZ at 18 and at 40 GHz. However, it is possible to optimise a larger number of frequencies and to apportion a greater or lesser priority as desired. Obviously, in case of a specific application the optimizer can be further finetuned to optimize at specific frequencies as well as having specific frequency dependent priorities on the performance. The results of this optimization are presented in Figure 10-e and -f. Here, it can be clearly seen that this provides a trade-of between performance at the lower frequency bound (12 GHz) whilst still providing good performance up to 40 GHz.

The reflector free form outline can be seen overlayed in Figure 9 as well. It can be seen that the serration length increased as well as the number of serrations is reduced against the 40 GHz optimization case. It is noted here that the serration to serration boundary of the last two optimization results is very sharp and might impose production issues, and thus requires further research on the impact if the contour sharpness is limited.

When comparing the resulting free form outline in Figure 9 it is also noted that the outer outline of this reflector resembles closely the outline of the optimized blended rolled edge reflector shown in Figure 8 (right). This suggests that QZ performance can be improved by adopting a curved reflector outline as opposed to the standard rectangular shape (*e.g.* Figure 8 (left)).

IV. Summary and Conclusions

In this work a full free form of the serrations outline based on the Superformula together with a squircle or Superformula based solid-serration boundary has been presented. It has been shown that both cases provide excellent CATR QZ performance, allowing the optimization of the QZ tailored to a specific customer requirement. Although not shown as a consequence of space, the simulations were repeated across a broad range of frequencies and it was found that the CATR QZ performance was unable to maintain the usual broad band nature of the design due to the high impact of the serration length and count on the frequency response. Thus the optimization was extended to allow for multi-frequency optimization and frequency dependent performance priority settings.

The optimization of the reflector outline shape provides considerable scope in terms of the freedom to tailor the reflector to any given predefined circumstances, *e.g.* chamber size and frequency range, providing a cost-effective and fully optimum performance to the customer.

References

[1] C. Parini, S. Gregson, J. McCormick, D. Janse van Rensburg and T. Eibert, Theory and Practice of Modern Antenna Range Measurements, 2nd Expanded Edition ed., vol. 1, London: IET Press, 2020.

[2] M. Dirix, S. Gregson and R. Dubrovka, "Genetic Optimization of Edge Treatmens of Single Offset Reflector Compact Antenna Test Ranges," in *AMTA Annual Meeting and Symposium*, Denver, CO, 2022.

[3] M. Dirix and S. Gregson, "Optimization of the Serration Outline Shape of a Single Offset Fed Compacte Antenna Test Range Reflector," in *EuCAP*, Düsseldorf, 2021.

[4] M. Dirix, S. Gregson and R. Dubrovka, "Genetic Evolution of the Reflector Edge Treatment of a Single Offset-Fed Compact Antenna Test Range for 5G New Radio Applications," in *AMTA Annual Meeting and Symposium*, Daytona Beach, Florida, 2021.

[5] S. Gregson, M. Dirix and R. Dubrovka, "Efficient Optimization of the Blended Rolled Edge of a Rectangular Single Offset Fed Compact Antenna Test Range Reflector Using Genetic Evoluation," in *EuCAP*, Madrid, 2022.

[6] J. Gielis, Inventing the Circle, Antwerpen: Geniaal bvba, 2003.

[7] E. Joy and R. Wilson, "Shaped Edge Serrations for Improved Compact Range Performance," in *AMTA Annual Meeting and Symposium*, 1987.

[8] C. Fong, "Analytical Methods for Squaring the Disc," in *International Cogress of Mathematicians, ICM*, Seoul, Korea, 2014.

[9] C. Parini, R. Dubrovka and S. Gregson, "Compact Range Quiet Zone Modelling: Quantitative Assesment using a Variety of Electromagnetic Simulation Methods," in *Loughborough Conference on Antennas and Propagation*, Loughborough, 2015.

[10] C. Parini, R. Dubrovka and S. Gregson, "CATR Quiet Zone Modelling and the Prediction of 'Measured' Radiation Pattern Errors: Comparison using a Variety of Electromagnetic Simulation Methods," in *AMTA 37th Annual Meeting & Symposium*, Long Beach California, 2015.

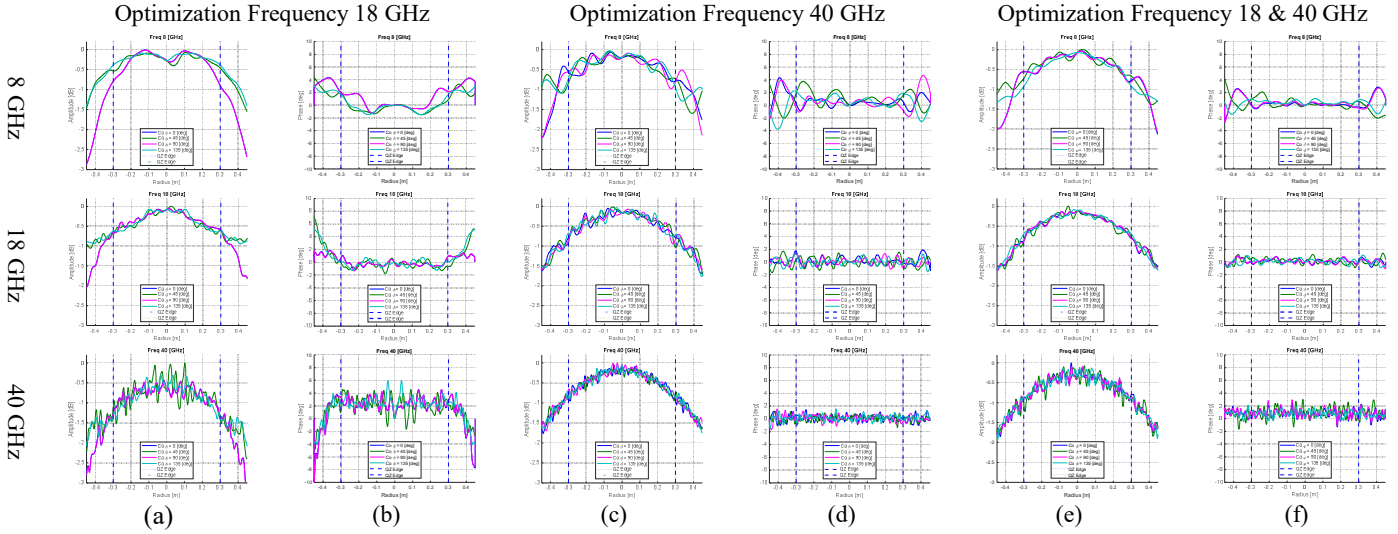

Fig. 10. Simulated results optimized at 18 GHz (a) amplitude- and (b) phase, optimized at 40 GHz (c) amplitude- and (d) phase, optimized simultaneously at 18 and 40 GHz (e) amplitude- and (f) phase. In each case copolar amplitude and phase QZ results are shown for 8 GHz, 18 GHz and 40 GHz.